Edinburgh Research Explorer

Snap Pump: A Snap-Through Mechanism for a Pulsatile Pump

Snap Pump: A Snap-through Mechanism for a Pulsatile Pump

Kazuki Arakawa[1], Francesco Giorgio-Serchi[2], and Hiromi Mochiyama[1]

Abstract—Pulsatile flow is widespread in nature, but replicating such impulsive periodic pumping routines with traditional rotary actuators is complex and energetically inefficient. We demonstrate the feasibility of an actuator capable of generating impulsive flow displacement by exploiting the bistable equilibrium of a simple mechanism. These kind of mechanisms, commonly known as snap-through mechanisms, offer the benefit of sudden release of elastic energy at the interface between two stable structural configurations. This property has been employed in certain actuators to drive abrupt motions of mechanical systems. Here, we use this principle to drive an inflation/deflation routine of a fluid-filled cavity, thus generating a peaked, pulsatile flow, comparable to that encountered in biological systems. Assessment of the various stages of actuation of this system shows that a sharp drop in the energy occurs from elastic to hydraulic work, highlighting the need for improved design elements involved in this stage of the actuation.

Index Terms—Soft robot applications, biologically-inspired robots, hydraulic/pneumatic actuators.

I. INTRODUCTION

Pulsatile flow is ubiquitous in nature as a mean to transfer fluid within a conduit. This is broadly defined as a flow driven by the periodic onset of pressure gradients which ultimately drive the displacement of finite volume of fluids at discrete time intervals. Pulsated flow regimes are encountered broadly in circulatory blood flow [1], but they are also prominent as a mean of propulsion for many aquatic organisms across diverse size scales [2]. Many variants of pulsatile pumps exist in nature, but the underlying working principle is common to all of these and entails an elastic hollow cavity capable of inflating and deflating, thus driving the periodic ingestion and expulsion of fluid through distinct apertures. Typical examples of such biological pumps are represented by the heart [3] and the mantle of cephalopods [4], which incidentally manifest a striking resemblance [5]. In the context of biomedical applications, and in particular in the design of artificial hearts,

very little work has been devoted to the design of more biological pulsating mechanisms [6], relying instead on robust centrifugal systems. Similarly, aquatic propulsion depends exclusively on continuously rotating propellers, despite the widespread evidence that organisms propelling themselves via pulse-jets benefit of unparalleled efficiency and unmatched manoeuvrability, [7], [8].

While traditional fluid displacement technologies has so far largely relied on continuous rotative mechanisms for the most part analogous to centrifugal pumps, the benefits associated with a discontinuous, periodic flow are currently pushing towards more biologically inspired solutions. Recent work on the role of the pulsatile nature of the flow in biological systems has highlighted its association with healthy cardiac activity [5], as well as with optimal swimming performances in several sea-dwelling organisms [5], [4]. This has remarkable implications in the design of biomedical and mechatronics systems whose purpose is to replicate the biological features of fluid transfer. A pivotal character of biologically inspired pumps is their capability to perform impulsive flow discharge, thus giving rise to highly asymmetric, period pulsation, i.e. defined by a slower inflow and a faster outflow, [9]. In the frame of aquatic propulsion this has obvious benefits due to the quadratic scaling of the jet thrust with the pump volume rate of change, [2]. In addition, recent work on the contribution to thrust from added-mass variation, [10], [11], further reinforces the argument in favour of impulsive fluid ejection during pulsation. This, however, remains a complex design feature, especially if intended for implementation in a small-scale, self-contained actuator. While commercial peristaltic pumps are indeed available, they are commonly associated with low-speed, low-volume flow displacement, making them unfit for replicating the impulsive fluid transfer mechanisms encountered in nature.

Recent work on the design of bioinspired pulsatile flow actuators has mainly revolved around their exploitation in the context of aquatic propulsion, [12], [13]. These designs are based on a constantly rotating driving unit connected to a reciprocating actuator whose output entails a harmonic fluid displacement, thus disregarding the chance to perform impulsive jets. Other designs are capable of generating non-harmonic flow routines, [14], but the chance to generate more impulsive pulsation still remains unsolved. In order to maximize flow speed and hence hydraulic power output, [15] resorts to a design based on sudden energy release of a fluid-filled elastic cavity. While this approach has the potential to magnify power output with respect to the nominal power of the driving unit, it also suffers from a slow process of charging

elastic potential energy, which dramatically constrains the potential for real-world operation of the system. The exploitation of abrupt elastic energy release represents a promising solution for the design of impulsive pulsatile flow mechanisms and there is also evidence that living organisms may exploit the elasticity of their tissues to maximize swimming efficiency, [16], [17], [8].

State-of-the-art compact impulse force generators can be found in researches of jumping robots. Sandia National Laboratory developed a jumping named Hopper which can leap up to the height of 9 m with a piston driven by a powerful internal combustion engine using liquid hydrocarbon as a fuel [18]. This amazing technology leads to a mobile robot named SandFlea of Boston Dynamics. This four-wheeled mobile robot can reach to the top of a building roof with one jump [19]. Tsukagoshi et al. proposed a two-wheeled mobile robot for rescue purposes, Leg-in-Rotor, which has an ability of 0.8 m jump using a pneumatic cylinder [20]. The most popular way to generating an impulse force with a compact mechanism is to utilize elastic bodies, that is, to store a potential energy to an elastic body and then release the stored energy instantaneously. We can find a wide variety of elastic impulse force generators. Usually, elastic bodies are used with electromagnetic motors The most classical elastic impulse force generator is to push, pull or twist a spring by an eccentric cam for releasing the stored energy of the spring, which is same in principle as the cam hummer invented by Leonardo da Vinci about 500 years ago. Scarfogliero et al. adopted this mechanism for a compact jumping robot, Grillo [21]. Kovac et al. succeeded to develope a 7 g miniature jumping robot which achieved 1.4 m jump based on this mechanism [22]. The most successful example using this classical elastic mechanism might be Jumping Sumo by Parrot, a radio-controlled robot toy [23]. This robot toy, actually a two-wheeled inverted pendulum, can move fast on a flat ground, and jump up to the height of 0.8 m. The collaboration research by Cho and Fearing invented a mobile and jumping robot, JumpRoACH, which can adjust the jumping height [24]. This light and small robot utilizes an elastic pantograph combined with an active clutch for a quick energy release, and has a capability of 0.72m jump with running. Each mechanism shown above has excellent properties as an impulse force generator, but is not suitable for a compact pump for generating pulsatile flows. While snap-through instabilities achieved by completely soft robots have been used for various functions including pumps [25], the obtained impulse force is expected to be much smaller than those of the examples above.

Here we propose to use a structurally bi-stable mechanisms as the driving unit of a pulsatile flow pump. These kind of systems, also referred to as a snap-through mechanisms or Snap Motors, have shown unique dynamical features associated with their capability to generate impulsive forces by exploiting the onset of steep gradients of elastic potential energy, [26], [27]. The insightful theoretical investigation of the snap-through phenomenon by a planar elastic catapult can be found in [28], [29].

The reminder of this paper introduces the design principles and operation of a pulse-flow pump based on a snap motor,
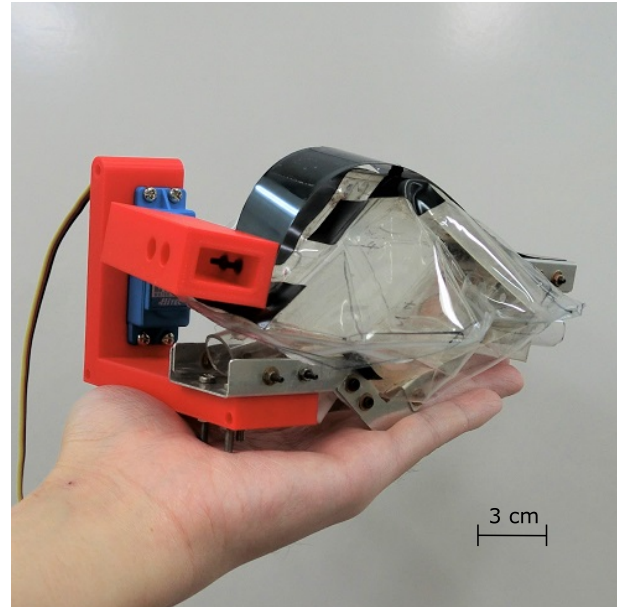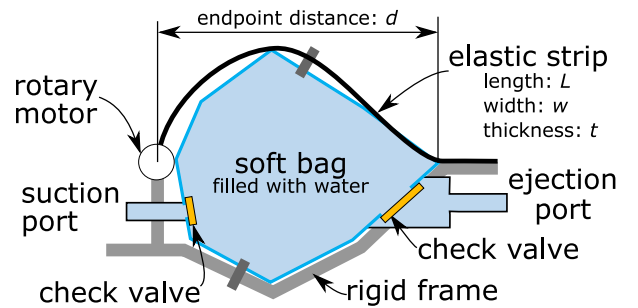

Fig. 1. The Snap Pump.

Fig. 2. Schematics of the snap-through mechanism.

which we will call a Snap Pump and demonstrate its suitability for implementation as a stand-alone actuator in the design of aquatic propulsors and artificial hearts.

II. SNAP PUMP DESIGN

A snap motor is an actuator that generates impulse force using snap-through buckling of an elastic strip. The working principle of the snap motor entails the progressive bending of an elastic strip by means of a rotary motor, Fig. 1 and Fig. 2. The elastic strip has a bi-stable equilibrium, so that the rotary actuator brings the strip to the buckling point, thus enabling it to snap from one stable configuration into the other, Fig. 3. These two stable configurations of the elastic strip correspond to the inflated and deflated states of the snap pump. The transition from one state to the other effectively drives the ingestion and expulsion of fluid, Fig. 4.

Fig.2 shows the mechanism of snap pump, fig.4 shows the cycle of the pump actuation.

Once assembled, the snap pump consists of the snap motor and a soft bag, locally connected to the elastic strip, which acts as the container for the displaced fluid. The soft bag is embedded with an ejection port and a suction port, which passively modulate the fluid inflow and outflow by means

of check valves, thus guaranteeing mono-directionality of the flow. The snap pump works by periodically undergoing upward and downward snap-through buckling of the elastic strip of the snap motor. The downward snap-through drives the collapse of the Soft Bag under the effect of the mechanical compression of the buckled elastic strip. We refer to the downward snap-through as snap-on. This occurs in coordination with the passive opening of the ejection port and closure of the suction port as a result of onset of pressure gradients along the flow line. The pressure difference between the inside and outside of the Soft Bag drives the issuing of fluid through the ejection port valve. During upward snap-through, the Soft Bag expands pulled by the reversed buckling of the elastic strip; the suction port opens, and water is sucked through the suction port. We refer to upward snap-through as snap-off. By cyclic repetition of the above routine the snap pump generates an intermittent, impulsive, pulsatile flow. A prototype of the assembled snap pump is shown in Fig.1 and Fig.5, while its collapsed and inflated configurations are shown in Fig. 3 and Fig. 4.

The elastic strip is made of SK85-CSPH (JIS) and its size is 135 mm long, 30 mm wide and 0.25 mm thick. The distance between the fixed position of the end point of the elastic strip and the rotation axis of the rotary motor is 90 mm. The rotary motor is a HS-5646WP (Hitec Multiplex Japan) and the whole prototype is mounted on a rigid aluminium frame for testing purposes. The motor is driven by a constant input voltage of 7V and position controlled to a target angle via Pulse Width Modulation (PWM) signal. In order to cause the alternated snap-on snap-off routine, two different target angles are cyclically commanded to the rotary motor. The Soft Bag is made of a vinyl sheet outside and styrene plates. Styrene plates are employed to prevent and limit wrinkling of the Soft Bag surface. Check valves consist of rectangular natural rubber sheets.
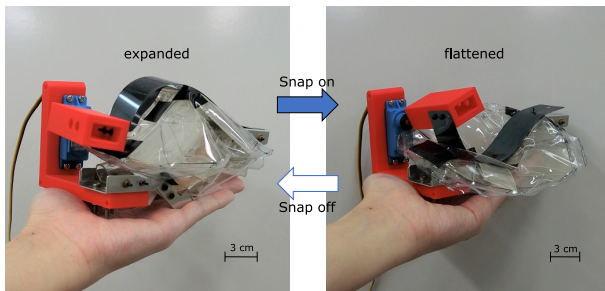

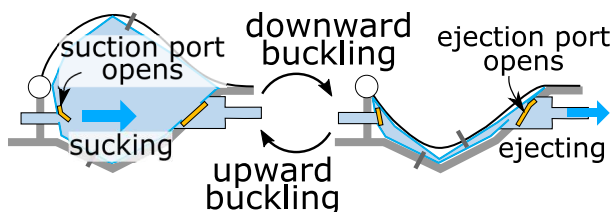Fig. 3. Bi-stable state transition of the Snap Pump: expanded and flattend.

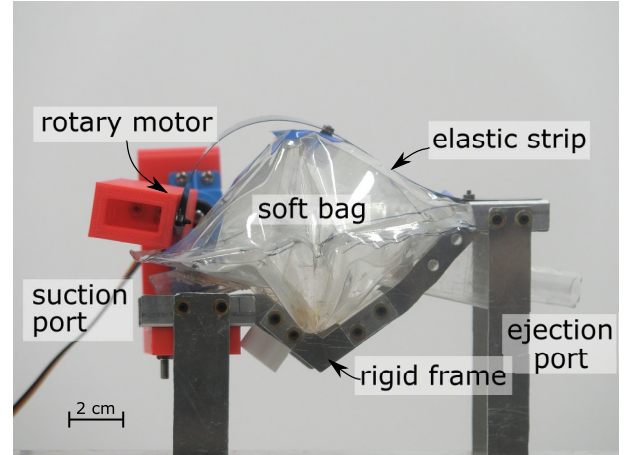Fig. 4. Schematic depiction of the actuation cycle of the pump.

Fig. 5. Side view of the prototype of the Snap Pump.

III. EXPERIMENT

In order to assess performance of this first pulsatile pump prototype, we record a set of key parameters throughout the actuation routine of the pump. The parameters employed are: electric current, flow rate through the inflow and outflow ports and pressure. These enable to derive three further metrics represented by the electric energy consumption, output work and pump efficiency. The experiment entails operating the pump at a constant, fixed, pulsation frequency, as dictated by the constant actuation routine of the snap motor. The set of metrics employed for establishing the performance of the prototype are also applied to a commercial pump as a mean of comparison of the newly introduced prototype.

A. Performance Metrics

The electric energy consumption E_{con} can be calculated by integrating the product of the voltage applied to the motor V_s and the motor current I_{motor} over the time period of one cycle of the snap motor T as,

$$E_{con} = \int_T V_s I_{motor} dt. \tag{1}$$

Here the output work of the snap pump is evaluated in two ways. One way, defined here as W_1, is to evaluate it based on the time integration of the sum of the fluid works at both the input and output ports. Each mechanical work is calculated by the product of a volume flow rate and a fluid pressure. This gives,

$$W_1 = \int_T (p_{in} Q_{in} + p_{out} Q_{out}) \, dt \tag{2}$$

where p_{in} and p_{out} are the water pressures at the input and output ports, and Q_{in} and Q_{out} are the volume flow rates at the input and output ports. Alternatively, fluid work can be estimated based on the kinetic energy required for delivering a finite amount of fluid with a mass m over a distance d with the average velocity v_{av} over the period T. This output work, refferred to as W_2, can thus be written by

$$W_2 = \frac{1}{2} m v_{av}^2 = \frac{1}{2} m \left(\frac{d}{T} \right)^2. \tag{3}$$
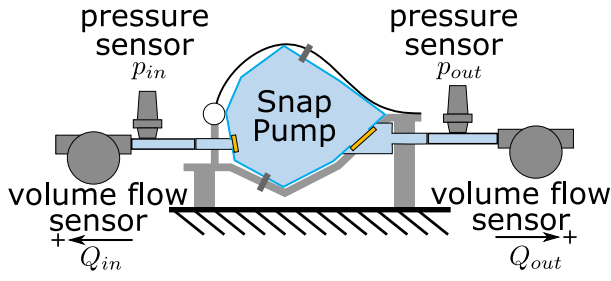
Fig. 6. Schematics of the apparatus, consisting of the pump and the sensors, for assessing the performance of the snap pump prototype.
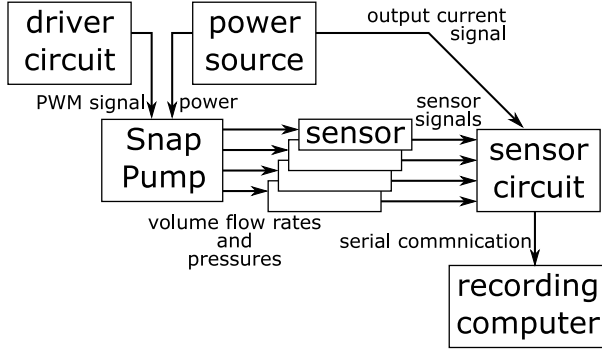

Fig. 7. Diagram of the apparatus.

Based on the above, two types of energy efficiency η_1 and η_2 respectively corresponding to W_1 and W_2 can be defined as follows,

$$\eta_1 = \frac{W_1}{E_{con}}, \tag{4}$$

$$\eta_2 = \frac{W_2}{E_{con}}. \tag{5}$$

B. Experimental Setup

Fig.6 shows an overview of the apparatus for measuring the motor current, the water pressures and volume flow rates at both the input and output ports in order to calculate the energy efficiency of the pump. Fig.7 shows a block diagram of the apparatus. The apparatus consists of a base, a power source (PMX18-5A, KIKUSUI), a circuit for driving the snap pump, two pressure sensors, two volume flow rate sensors and a circuit for the sensors. The pressure sensor is a KP1517G5-K ($\pm$ 5 kPa range, $\pm$ 0.5 %F.S. accuracy). The volume flow rate sensor is a SEN0217 ($1 \sim 30$ L/min range, $\pm$ 5 % accuracy). The power source is supplied with a constant voltage of 7 V, which represents the nominal operating current for the motor. Data transfer from the sensors is provided at 10Hz, sufficient for characterizing the current prototype. The hydraulic circuit entails an external water pool to which both ports of the snap pump are connected, thus ensuring consistent pressure conditions. The total length of the hydraulic circuit through the snap pump is 0.47 m.
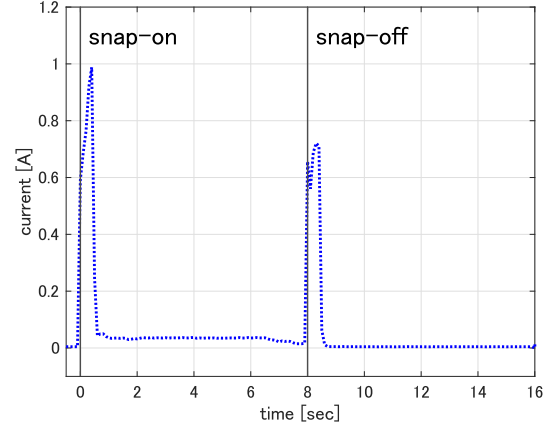

Fig. 8. Electrical current absorbed by the Snap Motor throughout pulsation cycle. Solid lines refer to the motor rotation commanded to drive the snap-through buckling of the elastic beam.
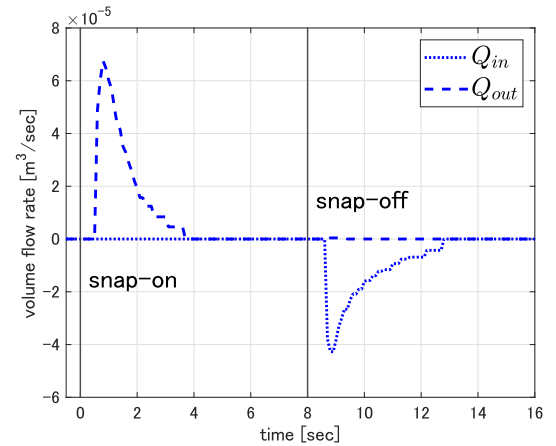
Fig. 9. Volume flow rate; the direction of the volume flow rate is defined as positive when aligned with the direction of flow out of the soft bag.

C. Experimental Results

The tests performed on the snap pump yield evidence of a clear pulsatile flow regime. This is characterized by a distinctive spike in flow rate associated with the abrupt expulsion of a finite volume of fluid under the impulse of the snap-through mechanism. Fig.8, Fig.9 and Fig.10 show the current, the volume flow rates and the pressures of the snap pump measured over a characteristic pulsation cycle of 16 seconds. The operation of the snap motor, i.e. the commanded changes of motor angle which drive the snap-through buckling, are indicated in Fig. 8, Fig. 9 and 10 by solid vertical lines.

From Fig.8, the spike in electrical current immediately after snap-on and snap-off can be observed. Based on the data reported in Fig. 8 and knowledge of the constant applied voltage, the electrical energy consumption for one cycle E_{con} is found to be 7.0 J. Unsteady volume flow rate evolution closely follows the electrical current signal, as reported in Fig.9. Flow rate manifests a very rapid variation after snap-on and snap-off, bringing evidence that a sharp pulsatile flow is successfully produced by the snap pump. It is worth noticing

Fig. 10. Time history of the pressure signal recorded at the inflow and outflow ports throughout a pulsation cycle consisting of a snap-on and a snap-off event.
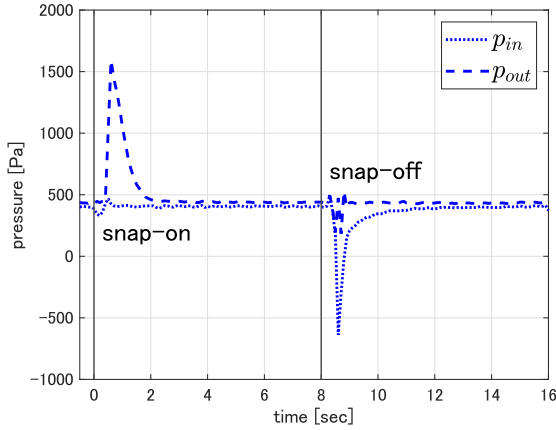
the time-delay between the instant when the snap motor is commanded and the sudden spike in flow rate (in either flow directions). This time delay corresponds exactly to the width of an impulse signal of the electrical current, indicating the characteristic time scale for the activation of the snap-through process with the present elastic strip. For the case examined in this experiment, the time necessary for ejecting the content of the soft bag is about 3.7s, while the time for ingesting the same amount of fluid is about 4.9s. Altogether, the minimum time required for a complete snap-through pumping cycle is 8.6s. The water volume expelled in a single pulsation is about 8.1×10^{-5} m^3 (i.e., 81 cc). Therefore, this snap pump has the ability to deliver 0.081 kg water for the total conduit length of 0.47 m in 8.6 s at an average speed $v_{av} = 0.055$m/s. The output work calculated based on kinetic energy W_2 is estimated at 1.2×10^{-4} J. Therefore, the energy efficiency in this case η_2 is 1.7 $\times 10^{-3}$ %. From Fig.10, we also can see a very rapid increase and decrease in pressure after snap-on and snap-off, respectively. The output work W_1 can be computed from the pressure data reported in Fig. 10 and it is estimated at 4.5×10^{-2}J. The energy efficiency in this case η_1 is 0.64 %.

D. Discussion

The work W_1 can be considered as the work done by the pump against the external fluid-pressure. Fig. 10 shows that the baselines of the input and output pressure are almost same, which means that the pump does not actually do any work on the fluid in the reservoirs in front of and behind the pump although the pump can still work against an elevated output pressure. In this respect, the recorded increase in pressure during snapping depicted in Fig. 10 represents internal processes associated to sudden increase of fluid inertia and viscous fluid resistance within the input and output tubes. We can employ this observation as an indication on how to make snap-off slower and snap-on faster, which was mentioned as a desirable feature for the purpose of propulsion. This can be achieved by designing the system such that a differential in fluid inertia and resistance arise between the input and output conduits, thus

giving rise to an asymmetric flow rate during the ingestion and expulsion stages of the pulsation.

On the other hand, W_2 can be considered as the useful work for generating thrust. This represents a more meaningful metric when assessing the effectiveness of the snap pump in the frame of pulsed-jet aquatic propulsion. According to the definition of W_2, the reduction of flow resistance across the inflow and outflow conduits will also participate in increasing this quantity.

In this respect, it is worth noticing that active control of the differential nozzle diameter during ingestion and expulsion of a jet is commonly observed in living specimen of pulsed-jetting organisms, [30]. This provides further evidence that such mechanism may constitute a viable strategy to increase the net cycle-averaged power of this kind of pulsatile systems.

IV. ENERGY FLOW ANALYSIS

For better understanding the proposed snap pump, we analyze the energy flow for the snap pump system. The snap pump system temporarily stores the elastic energy in the elastic strip, and releases the part of this elastic energy by snap-through buckling for generating a pulsatile flow. This released elastic energy can be estimated by quasi-static simulation of largely deformable elastic rods [31] based on the rod theory [32], [33].

Fig.11 shows the elastic energy stored during the shape transition. The horizontal axis denotes the angle of the motor which is fixed to one end of the elastic strip. According to this motor angle, the shape of the elastic strip changes. The elastic energy of the elastic strip E_r can be calculated by

$$E_r = \frac{1}{2} \int_0^L k\theta(\sigma)^2 d\sigma \qquad (6)$$

where L is the length of the rod, and k is the bending stiffness which is a product of the Young's modulus and the moment of inertia of the rod cross section. For the elastic strip used in the prototype, $L = 135$ mm and $k = 8.8 \times 10^3$ N/mm^2. σ is the arc length parameter, and $\theta(\sigma)$ is the curvature of the statically-balancing rod at σ. In the simulation, the rod is approximated by a serial-chain of rigid links connected with N joints. Then, the elastic energy of the elastic strip E_r can be calculated approximatedly by

$$E_r \approx \frac{1}{2} \sum_{i=1}^{N} k_d \theta_i^2 \qquad (7)$$

where θ_i is the relative angle of i-th adjacent links, $k_d := kN/L$ is discretized bending stiffness. In this energy flow analysis, N is set to 30. See [31], [33] for more detail about the quasi-static shape computation. From this quasi-static simulation result, we can see that the released elastic energy for one snap-through buckling is 0.47 J, which means that the total released elastic energy for one cycle is 0.94 J, if both snap-on and snap-off are accounted for in one cycle. The step-by-step energy efficiency of the snap pump are summarized in Table.I.

The first step from the electrical energy consumption E_{com} to the released elastic energy E_r is related to the energy
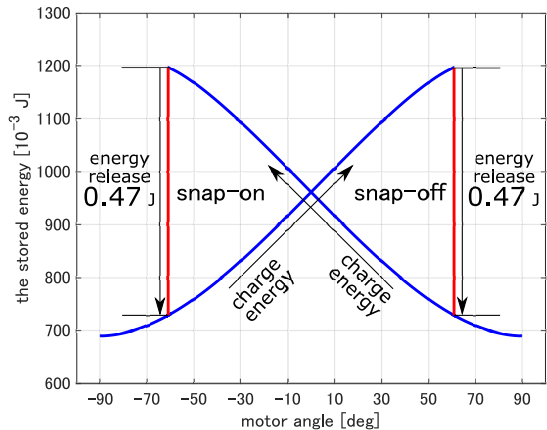
Fig. 11. The stored elastic energy during snap-through buckling.

efficiency of the snap motor itself. The energy efficiency of this step is 13.4 %. The snap motor employed for this snap pump rotates the output axis back and forth. This type of snap motors is mechanically simple, but not efficient. One improvement of this design to achieve a better efficiency lies in utilizing a slider-crank mechanism such as that previously used for a jumping robot [27] where the electric motor is required to rotates in one way only.

The second step entails the transfer from the released elastic energy E_r to the output fluid work W_1 and is largely dependent on the soft bag deformations i.e., flattened and expanded, by the snap-through mechanism. The energy efficiency of this step is only 4.8 %. This appears to represent the major limitation to an efficient energy transfer from from the mechanical system to the fluid. Some elements which are responsible for this are the discrete, localized connection points between the elastic strip (flexible in some direction but very stiff in other directions) and the soft bag. This causes the soft bag to not collapse entirely, thus preventing part of its content from being ejected from the cavity. All this suggests that there are several design features which can be largely ameliorated to facilitate energy transmission across the system.

TABLE I
ENERGY FLOW

Step	Energy (J)	Step-by-step Efficiency (%)
E_{con}	7.0	-
E_r	0.94	13.4%
W_1	4.5×10^{-2}	4.8%

V. CONCLUSIONS

In this paper, a new pump for generating pulsatile flow is proposed. This mechanisms uses a motor to trigger the buckling of an elastic strip, which in turn drives the deflation and inflation of a fluid-filled deformable chamber. The recursive operation of this simple mechanisms drives the onset of impulsive displacement of finite slug of fluids, demonstrating the onset of a distinctively pulsatile flow regime.

The highly impulsive nature of the flow, while desirable for more biologically inspired application, makes it difficult

to assess the performance of this pump with respect to equivalent commercial systems. However, a first evaluation of the performance of this mechanisms is assessed based on its efficiency. This metric is biased towards more steady-state pumping systems; nonetheless its comparison with a diaphragm pump operating at quasi-steady regime shows very similar performances.

By evaluating the process of energy transfer through the various elements of the proposed mechanism, it is shown that the limiting factors lie both in the transfer from electrical to elastic energy and from elastic potential to hydraulic power. This enables to focus the future design improvements on two key design elements. First, the operation of the prototype requires repeated reversals of the rotary motor's direction of rotation, which requires the rotary motor to start and stop repeatedly. Generally, rotary motors require more energy to start and stop than they do in steady-state rotation. Therefore, we aim to use a mechanism such as that shown in [27] to cause repeated snap-through buckling by constant rotation of the rotary motor. This improvement can relieve from the energy required for starting and stopping the motor. Secondly, improvements in the fluid-filled collapsible cavity are necessary to improve overall efficiency. A significant improvement may be promoted by a better connection between the buckling unit and the deformable cavity. One further improvement lies with the check valves. A rubber seat is currently used for check valve operation, but this requires a lot of energy to open wide due to the elasticity of the rubber seat. Using a mechanical check valve with hinges instead of a rubber seat can reduce energy loss. In addition, the sharp edges of the suction and ejection ports may cause significant viscous losses, resulting in drastic reduction in hydraulic power.

Despite the low estimated efficiencies and its design limitations, this prototype demonstrates the feasibility of producing biologically-looking pulsatile flow regimes by relying on a lightwheight, self-contained, simple mechanical system. This paves the way to further development of this design for its future application in the context of biomedical and bioinspired propulsion technology.

APPENDIX

For the sake of better understanding of the proposed snap pump, the same experimental setup is also tested with a commercial diaphragm pump, i.e. the DPE-800 [34] from NITTO KOHKI CO., LTD. This pump represents a suitable comparison against the snap pump because it also employs a pumping routine based on the pressurization of a fluid-filled chamber under the effect of an oscillating diaphragm. The difficulty in establishing a comparison between the snap pump and the DPE-800 stems from the latter operating at relatively high pulsation frequencies over small fluid volumes, ultimately yielding a quasi-steady flow rate. Additional differences with the snap pump lie in the operating voltage of the DPE-800 at 17V, and on the hydraulic circuit through this pump being 0.99m.

An analogous set of results achieved with the commercial diaphragm pump is reported in Fig.12, Fig.13 and Fig.14,
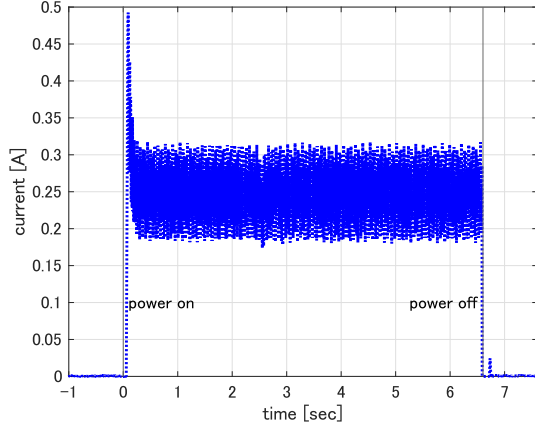
Fig. 12. Electric current of the DPE-800 pump at constant 17V operation. operation

Fig. 14. Pressure at suction and ejection ports during operation with the DPE-800 pump.
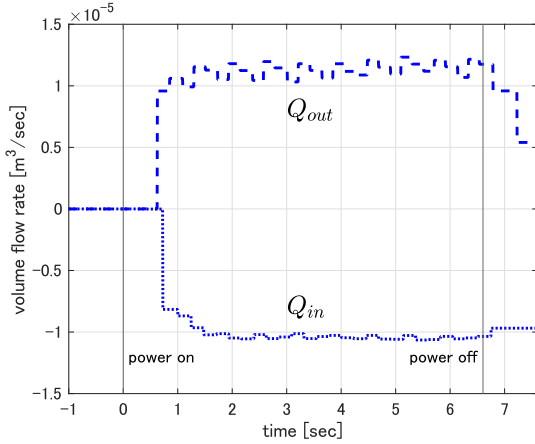

Fig. 13. Volume flow rate of the DPE-800 pump.

respectively for the electric current, the volume flow rate and the pressure. From Fig.12, we can see that a noisy electrical current flows for this liquid pump. The average current is 0.25A. Considering 17V applied voltage and this current average, the power consumption of this commercial pump is 4.25W. By applying these estimates for a testing period analogous to the minimum characteristic cycle of the snap pump $T = 8.6$s, the total electrical energy consumption of the DPE-800 pump is 36.6 J. From Fig.13, the flow rate generated by the diaphragm pump shows a distinctive step flow-rate signal followed by a sawtooth shape. The average value is 0.96×10^{-5} m^3/s. For the period (i.e., T=8.6 s), this commercial pump delivers the water with the volume of 8.26×10^{-5} m^3 (i.e., 82.6 cc). Considering the total conduit length of 0.99 m, the average flow speed is 0.115 m/s. The output work calculated from the kinetic energy W_2 is 5.46 $\times 10^{-4}$ J. Therefore, the energy efficiency in this case η_2 for this commercial pump is 1.5 $\times 10^{-3}$ %. From Fig.14, we can see very noisy pressure signals. The average absolute values of p_{in} and p_{out} are 580 and 4300 Pa, respectively. The output work for fluid work W_1 for this commercial pump is 0.415 J and the energy efficiency in this case η_1 is 1.13 %.
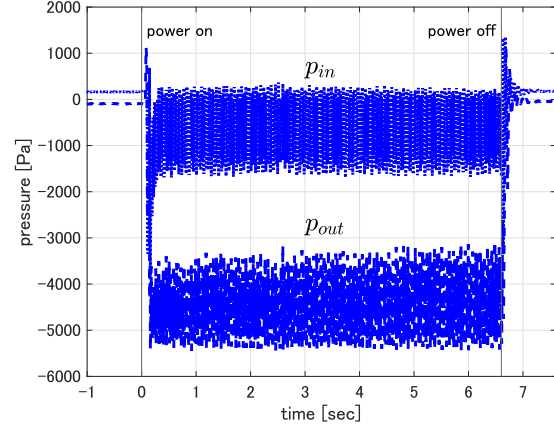
The comparison result can be summarized in Table.II. The energy efficiency due to fluid work η_1 for the snap motor is about a half of that for the commercial pump. However, the energy efficiency calculated from the kinetic energy of the water delivered by the snap pump is better than that by the commercial pump. The performance of the snap pump is comparable to the commercial pump in spite of being light. Note that the weight of the snap pump is just a half of the commercial pump for this comparison.

TABLE II
COMPARISON BETWEEN THE SNAP PUMP AND A COMMERCIAL PUMP

	Snap pump	DPE-800
weight (g)	182	380
the electrical energy consumption E_{con}(J)	7.0	36.6
the output work W_1(J)	0.045	0.415
the energy efficiency η_1 (%)	0.64	1.13
the output work W_2(10^{-4} J)	1.2	5.5
the energy efficiency η_2 (10^{-4}%)	1.7	1.5

REFERENCES

[1] Y. C. Fung, *Biomechanics – Motion, flow, stress and growth.* Springer-Verlag, 1990.
[2] W. Johnson, P. D. Soden, and E. R. Trueman, "A study in met propulsion: an analysis of the motion of the squid, *Loligo Vulgaris*," *Journal of Experimental Biology*, vol. 56, pp. 155–165, 1972.
[3] L. P. Dasi, H. A. Simon, P. Sucosky, and A. P. Yoganathan, "Fluid mechanics of artificial heart valves." *Clinical and experimental pharmacology & physiology*, vol. 36 2, pp. 225–37, 2009.
[4] I. K. Bartol, P. S. Krueger, W. J. Stewart, and J. T. Thompson, "Hydrodynamics of pulsed jetting in juvenile and adult brief squid *Lolliguncula brevis*: evidence of multiple jet 'modes' and their implications for propulsive efficiency," *Journal of Experimental Biology*, vol. 212, pp. 1889–1903, 2009.
[5] J. Dabiri, "Optimal vortex formation as a unifying principle in biological propulsion," *Annual Review of Fluid Mechanics*, vol. 41, pp. 17–33, 2009.
[6] N. Cohrs, A. Petrou, M. Loepfe, M. Yliruka, C. Schumacher, X. Kohll, C. Starck, M. Schmid Daners, M. Meboldt, V. Falk, and W. Stark, "A soft total artificial heart-first concept evaluation on a hybrid mock circulation," *Artificial organs*, vol. 41, 07 2017.
[7] I. K. Bartol, P. S. Krueger, J. T. Thompson, and W. J. Stewart, "Swimming dynamics and propulsive efficiency of squids throughout ontogeny," *Integrative and Comparative Biology*, vol. 48, no. 6, pp. 720–733, 2008.

[8] B. J. Gemmell, J. H. Costello, S. P. Colin, C. J. Stewart, J. O. Dabiri, D. Tafti, and S. Priya, "Passive energy recapture in jellyfish contributes to propulsive advantage over other metazoans," *Proceedings of the National Academy of Sciences*, vol. 110, no. 44, pp. 17 904–17 909, 2013.

[9] I. K. Bartol, M. R. Patterson, and R. Mann, "Swimming mechanics and behavior of the shallow-water brief squid *Lolliguncula brevis*," *Journal of Experimental Biology*, vol. 204, pp. 3655–3682, 2001.

[10] F. Giorgio-Serchi and G. D. Weymouth, "Drag cancellation by added-mass pumping," *Journal of Fluid Mechanics*, vol. 798, 2016.

[11] ——, "Underwater soft robotics, the benefit of body-shape variations in aquatic propulsion," in *Soft Robotics: Trends, Applications and Challanges*, ser. Biosystems & Biorobotics. Springer, 2016, vol. 17, pp. 37–46.

[12] M. Krieg and K. Mohseni, "Dynamic modeling and control of biologically inspired vortex ring thrusters for underwater robot locomotion," *IEEE Transactions on Robotics*, vol. 26, pp. 542–554, june 2010.

[13] F. Giorgio-Serchi, A. Arienti, and C. Laschi, "Underwater soft-bodied pulsed-jet thrusters: Actuator modeling and performance profiling," *International Journal of Robotics Research*, 2016.

[14] P. S. Krueger and M. Gharib, "The significance of vortex ring formation to the impulse and thrust of starting jet," *Physics of Fluid*, vol. 15, pp. 1271–1281, 2003.

[15] F. Giorgio-Serchi, A. K. Lidtke, and G. D. Weymouth, "A soft aquatic actuator for unsteady peak power amplification," *IEEE/ASME Transactions on Mechatronics*, vol. 23, no. 6, pp. 2968–2973, Dec 2018.

[16] J. M. Gosline and R. E. Shadwick, "The role of elastic energy storage mechanisms in swimming: an analysis of mantle elasticity in escape jetting in squid, *Loligo opalescens*," *Canadian Journal of Zoology*, vol. 61, pp. 1421–1431, 1983.

[17] P. S. Macgillavray, E. J. Anderson, G. M. Wright, and M. E. Demont, "Structure and mechanics of the squid mantle," *Journal of Experimental Biology*, vol. 202, pp. 683–695, 1999.

[18] "Sandia National Laboratories news releases, 2000." https://www.sandia.gov/media/NewsRel/NR2000/hoppers.htm, accessed: 2019-07-24.

[19] "Boston Dynamics sandflea, 2012." https://www.bostondynamics.com/sandflea, accessed: 2019-07-24.

[20] H. Tsukagoshi, M. Sasaki, A. Kitagawa, and T. Tanaka, "Design of a higher jumping rescue robot with the optimized pneumatic drive," 4 2005, pp. 1288–1295.

[21] U. Scarfogliero, C. Stefanini, and P. Dario, "Design and development of the long-jumping "grillo" mini robot," 5 2007, pp. 467–472.

[22] M. Kovac, M. Fuchs, A. Guignard, J. Zufferey, and D. Floreano, "A miniature 7g jumping robot," 5 2008, pp. 373–378.

[23] T. Chong, "Parrot's mini quadrotor and jumping robot to hit stores in august," IEEE Spectrum, 2014. https://spectrum.ieee.org/automaton/robotics/home-robots/parrot-minidrones-rolling-spider-jumping-sumo, accessed: 2019-07-25.

[24] G.-P. Jung, C. S. Casarez, J. Lee, S.-M. Baek, S.-J. Yim, S.-H. Chae, R. S. Fearing, and K.-J. Cho, "Jumproach: A trajectory-adjustable integrated jumping-crawling robot," *IEEE/ASME Trans. on Mechatronics*, vol. 24-3, pp. 947–958, 2019.

[25] Z. Li, J. Zhu, C. C. Foo, and C. H. Yap, "Snapping of elastic strips with controlled ends," *APPLIED PHYSICS LETTERS*, vol. 111, pp. 212 901–1–5, 2017.

[26] H. Mochiyama, M. Watari, and H. Fujimoto, "A robotic catapult based on the closed elastica and its application to robotic tasks," in *Proceedings of the 2007 IEEE/RSJ International Conference on Intelligent Robots and Systems (IROS2007)*, 10 2007, pp. 1508–1513.

[27] T. Tsuda, H. Mochiyama, and H. Fujimoto, "Quick stair-climbing using snap-through buckling of closed elastica," in *2012 International Symposium on Micro-NanoMechatronics and Human Science (MHS)*, Nov 2012, pp. 368–373.

[28] C. Armanini, F. Dal Corso, D. Misseroni, and D. Bigoni, "From the elastica compass to the elastica catapult: an essay on the mechanics of soft robot arm," *Proc. R. Soc. A.*, vol. 473:20160870, pp. 1–23, 2017.

[29] A. Cazzolli and F. Dal Corso, "Snapping of elastic strips with controlled ends," *International Journal of Solids and Structures*, vol. 162, pp. 285–303, 2019.

[30] D. J. Staaf, W. F. Gilly, and M. W. Denny, "Aperture effects in squid jet propulsion," *Journal of Experimental Biology*, vol. 217, no. 9, pp. 1588–1600, 2014. [Online]. Available: https://jeb.biologists.org/content/217/9/1588

[31] H. Mochiyama, A. Kinoshita, and R. Takasu, "Impulse force generator based on snap-through buckling of robotic closed elastica: Analysis by quasi-static shape transition simulation," 11 2013, pp. 4583–4589.

[32] S. Antman, *Nonlinear problems of elasticity, 2nd Ed.* Springer, 2004, vol. 1.

[33] H. Mochiyama, "The elastic rod approach toward system theory for soft robotics," in *Proceedings of the 2020 IFAC World Congress*, 7 2020, p. 6 pages.

[34] "NITTO KOHKI CO., LTD. detailed technical specifications on nitto kohki linear poston air compressors," http://nitto-kohki.meclib.jp/Lk001/book/#target/page_no=93, accessed: 2020-10-01.